


# SCIENTIFIC DATA

OPEN

DATA DESCRIPTOR

## High-resolution and bias-corrected CMIP5 projections for climate change impact assessments

Carlos Navarro-Racines<sup>1,2</sup>, Jaime Tarapues<sup>1,2</sup>, Philip Thornton<sup>2,3</sup>, Andy Jarvis<sup>1,2</sup> & Julian Ramirez-Villegas<sup>1,2,4\*</sup> 

Projections of climate change are available at coarse scales (70–400 km). But agricultural and species models typically require finer scale climate data to model climate change impacts. Here, we present a global database of future climates developed by applying the delta method—a method for climate model bias correction. We performed a technical evaluation of the bias-correction method using a ‘perfect sibling’ framework and show that it reduces climate model bias by 50–70%. The data include monthly maximum and minimum temperatures and monthly total precipitation, and a set of bioclimatic indices, and can be used for assessing impacts of climate change on agriculture and biodiversity. The data are publicly available in the World Data Center for Climate (WDCC; [cera-www.dkrz.de](http://cera-www.dkrz.de)), as well as in the CCAFS-Climate data portal (<http://ccafs-climate.org>). The database has been used up to date in more than 350 studies of ecosystem and agricultural impact assessment.

### Background & Summary

There is a variety of methods to project the impacts of climate change on agriculture and biodiversity. This diversity arises, at least in part, from the difficulty to couple local-scale agricultural or species distribution and abundance models with General Circulation Model (GCM) projections, which are inherently uncertain<sup>1–3</sup>. GCMs can only model earth processes in coarse grid-cells, which are unsuitable for local agricultural studies<sup>4,5</sup>. Most impact models for agriculture and biodiversity require high-resolution environmental data<sup>6,7</sup>.

Some authors (e.g. refs. <sup>8–10</sup>) argue that original GCM resolutions should be kept so as not to bias or alter the physical plausibility of GCMs. Nevertheless, agricultural and natural landscapes have large spatial variations, particularly in the tropics, where orography, climate (especially precipitation), soils and crop management, vary across small distances<sup>11</sup>. The vast majority of agricultural and biodiversity researchers have used downscaling in impact studies<sup>6,12</sup> (but see refs. <sup>13,14</sup>). This is because conservation plans, niche models, crop models, and biodiversity evaluation require high resolution inputs. Downscaling and bias correction of climate model output produces data that allows local rather than regional or global projections of climate change and its impacts<sup>15,16</sup>. Planning, modeling and monitoring can therefore be at municipality, watershed or other sub-national scales<sup>17–21</sup>.

Downscaling techniques range from smoothing and interpolation of GCM anomalies<sup>19</sup>, to statistical modeling, neural networks, and regional dynamical climate modelling<sup>22</sup>. They differ in accuracy, output resolution, computational requirements and climatic science robustness. Dynamical and statistical downscaling are the most frequently used techniques to downscale GCMs for agricultural impact studies<sup>23,24</sup>. Bias-correction, on the other hand, focuses on using different types of statistical techniques to make the climate model output more realistic, and, in many cases (i.e. when observations are available at high spatial resolution), also of greater spatial resolution<sup>15,25</sup>.

Dynamical downscaling uses Regional Climate Models (RCMs) to increase the resolution of climate projections, with boundary and initial conditions from a GCM as inputs<sup>26–28</sup>. RCMs consider more detailed specifications of land use and water bodies, simulate mesoscale processes in more detail than GCMs, and, in some cases, are capable of explicitly resolving convective rainfall processes<sup>29,30</sup>. RCMs are computationally expensive, and require physical understanding of the climate system, time and storage to obtain a single scenario-by-period output<sup>21</sup>. RCM outputs have been made available recently through the Coordinated Regional Climate Downscaling Experiment (CORDEX)<sup>31</sup>. However, given their computational cost, only a handful of RCM–GCM combinations

<sup>1</sup>International Center for Tropical Agriculture (CIAT), Cali, Colombia. <sup>2</sup>CGIAR Research Program on Climate Change, Agriculture and Food Security (CCAFS), c/o CIAT, Cali, Colombia. <sup>3</sup>International Livestock Research Institute (ILRI), Nairobi, Kenya. <sup>4</sup>School of Earth and Environment, University of Leeds, Leeds, UK. \*email: [j.r.villegas@cgiar.org](mailto:j.r.villegas@cgiar.org)

can realistically be used to produce future high-resolution climate change projections<sup>32,33</sup>. Moreover, RCM outputs are also subject to climate model error from both the structure of the RCM and the boundary conditions of the driving GCM<sup>30,34</sup>.

Statistical downscaling (SD) is an easier and computationally less expensive method to develop climate change projections with high spatial resolution<sup>35</sup>. SD typically consists of two steps, (i) developing a statistical relationship between local climate variables and large-scale predictors, and (ii) the application of those statistical models onto future GCM output to derive future downscaled data<sup>36</sup>. SD assumes that climates will only change at coarse scales and that relationships between variables at local scale remain relatively constant in the future period<sup>30,36</sup>. Bias correction (BC) is yet simpler than SD, and is typically implemented by applying a ‘change factor’ or ‘delta’ derived from a GCM onto the historical observations<sup>15,35</sup>. BC can also be implemented by applying a ‘nudging’ factor to the climate model output, or by quantile-mapping of climate model outputs onto observations<sup>16,37</sup>. Since no GCM is a perfect representation of the true climate, BC seeks to correct those attributes in the climate model output that are known or hypothesized to be important for impacts modeling<sup>4,15,38</sup>.

Here, we used BC to develop the CCAFS-Climate global database of bias corrected climate change projections. To develop the database, we applied the delta method (a simple BC) to 35 Coupled Model Intercomparison Project Phase 5 (CMIP5) models<sup>39</sup>, and four representative concentrations pathways (RCPs)<sup>40</sup>. We used the delta method since we focus on providing data for 30-year mean climate conditions, and because the method has already been shown to be robust to correct mean climate conditions in other regions<sup>15</sup>. For each GCM, we used the 30-year future periods named as 2030s (2020–2049), 2050s (2040–2069), 2070s (2060–2089) and 2080s (2070–2099) and three climate variables (mean monthly maximum and minimum temperatures and monthly rainfall). We used the WorldClim global climate database<sup>11</sup> as the reference set of observations for the historical period. The database is freely available through the World Data Center for Climate (WDCC; [cera-www.dkrz.de](http://cera-www.dkrz.de))<sup>41</sup>, as well as through the CCAFS-Climate data portal (<http://ccafs-climate.org>). We evaluate the method to quantify the advantages of using bias-corrected climate data in comparison with the original GCM outputs, using a perfect sibling framework (see Methods). Furthermore, we summarize existing applications of the high-resolution gridded datasets produced here in environmental studies characterizations to assess the impacts of climate change on agricultural production, biodiversity, conservation, and water resources. Finally, we discuss the assumptions and limitations in the methods and data.

## Methods

CCAFS-Climate was produced by bias-correcting the original GCM outputs using spatial interpolation of the anomalies or deltas (differences between future and current climates). To this aim, anomalies (‘deltas’) are first calculated using GCM output as the difference between future and historical periods, and then interpolated onto a 30 arc-s grid. We then applied the interpolated anomalies to the baseline climate of the WorldClim high resolution (30 arc-s) surfaces<sup>11</sup>. This method is called delta change or change factor<sup>42,43</sup> (DC). Our implementation of DC seeks to correct the modeled mean climate from the climate models, which is a critical aspect in understanding crop and species distributions and productivity under climate change<sup>44,45</sup>, while also providing results at high spatial resolution.

**Data acquisition.** *Present-day observed climatology.* We used the high spatial resolution (30 arc-s, ~1 km at the Equator) climate datasets of WorldClim<sup>11</sup>. We chose WorldClim due to its high spatial resolution, wide use (i.e. more than 15,000 citations), and quality<sup>11</sup>. WorldClim used data from more of 47,000 weather stations from 1950–2000 worldwide as input to produce interpolations. WorldClim used the thin-plate splines algorithm<sup>46</sup> to interpolate mean monthly maximum and minimum temperatures, and monthly precipitation. There are other global datasets for both temperature and precipitation<sup>47</sup>, but they use fewer locations or have coarser spatial resolution. Moreover, WorldClim compares well to other global datasets, especially in areas of high weather station density<sup>11,48,49</sup>.

*General circulation models data.* The Coupled Model Intercomparison Project Phase 5 (CMIP5)<sup>39</sup>, coordinated by the World Climate Research Programme in support of the IPCC Fifth Assessment Report (AR5)<sup>50</sup>, provides simulations from state-of-the-art GCMs. CMIP5 provides, for a large number of models, climate projections for all four Representative Concentration Pathways (RCPs)<sup>39</sup>.

We used present day simulations (1961–1990) and future projections (2010–2100) of global climate at original GCM resolution (70–400 Km) from a total of 35 GCMs, and all RCPs, namely, RCP 2.6, 4.5, 6.0 and 8.5 (Table 1)<sup>40</sup>. GCM data included monthly time series of maximum temperature, minimum temperature and precipitation flux. All GCM data were downloaded from the CMIP5 web data portal at <https://esgf-node.llnl.gov/projects/cmip5/>. Not all GCM-by-RCP combinations were available (see Table 1).

**Delta method downscaling.** The DC approach presented here is a simple form of BC in which a change factor or ‘delta’ is derived from the GCM, and then added onto the observations (WorldClim). The purpose of our dataset is to provide a bias-corrected and high-resolution representation of the mean climates, and for this reason we employ the DC approach. The change factor is defined as the difference between the long-term (30-year) mean of a climate variable in the future and the historical period. The method comprises the following steps: (1) calculation of 30-year averages for present-day simulations and 4 future periods; (2) calculation of anomalies as the absolute difference between future and present day values in temperatures (minimum and maximum) and proportional differences in total precipitation; (3) interpolation of these anomalies using centroids of GCM grid cells as points for interpolation; and (4) addition of the interpolated gridded data to the current climates from WorldClim (Fig. 1).

Using the full present-day monthly time-series from the GCM (Sect 0), we thus calculated 30-year means as a baseline (1961–1990), for each GCM and variable. Next, we calculated the 30-year means for each RCP and

| Model (Reference)                  | Institute   | RCP   |     |     |     |
|------------------------------------|---|---|-----|-----|-----|
|                                    |   | 2.6   | 4.5 | 6.0 | 8.5 |
| BCC-CSM1.1 <sup>91-93</sup>        | Beijing Climate Center, China Meteorological Administration   | O   | O   | O   | O   |
| BCC-CSM1.1(m) <sup>91-93</sup>     |   | O   | O   | O   | O   |
| BNU-ESM <sup>94</sup>              | Beijing Normal University   | O   | O   | X   | O   |
| CCCMA-CanESM2 <sup>95,96</sup>     | Canadian Centre for Climate Modelling and Analysis  | O   | O   | X   | O   |
| CESM1-BGC <sup>97,98</sup>         | National Science Foundation, Department of Energy, National Center for Atmospheric Research                                 | X   | O   | X   | O   |
| CESM1-CAM5 <sup>97</sup>           |   | O   | O   | O   | O   |
| CNRM-CM5 <sup>99</sup>             | Centre National de Recherches Meteorologiques and Centre Europeen de Recherche et Formation Avancees en Calcul Scientifique | O   | O   | X   | O   |
| CSIRO-ACCESS1.0 <sup>100,101</sup> | Commonwealth Scientific and Industrial Research Organization (CSIRO) and Bureau of Meteorology (BOM), Australia             | X   | O   | X   | O   |
| CSIRO-ACCESS1.3 <sup>100,101</sup> |   | X   | O   | X   | O   |
| CSIRO-Mk3.6.0 <sup>102</sup>       | Queensland Climate Change Centre of Excellence and Commonwealth Scientific and Industrial Research Organization             | O   | O   | O   | O   |
| EC-EARTH <sup>103</sup>            | European Centre for Medium-Range Weather Forecasts (ECMWF)  | X   | X   | X   | O   |
| FIO-ESM <sup>104</sup>             | The First Institute of Oceanography, State Oceanic Administration, China  | O   | O   | O   | O   |
| GFDL-CM3 <sup>105,106</sup>        | NOAA Geophysical Fluid Dynamics Laboratory  | O   | O   | O   | O   |
| GFDL-ESM2G <sup>107</sup>          |   | O   | O   | O   | O   |
| GFDL-ESM2M <sup>107</sup>          |   | O   | O   | O   | O   |
| GISS-E2H <sup>108,109</sup>        | NASA Goddard Institute for Space Studies USA  | O   | X   | O   | O   |
| GISS-E2HCC <sup>108,109</sup>      |   | X   | O   | X   | X   |
| GISS-E2R <sup>108,109</sup>        |   | O   | O   | O   | O   |
| GISS-E2RCC <sup>108,109</sup>      |   | X   | O   | X   | X   |
| INM-CM4 <sup>110</sup>             |   | Institute of Numerical Mathematics of the Russian Academy of Sciences | X   | O   | X   |
| IPSL-CM5A-LR <sup>111</sup>        | Institut Pierre Simon Laplace   | O   | O   | O   | O   |
| IPSL-CM5A-MR <sup>111</sup>        |   | O   | O   | X   | O   |
| IPSL-CM5B-LR <sup>111</sup>        |   | X   | X   | X   | O   |
| LASG-FGOALS-G2 <sup>112</sup>      | Institute of Atmospheric Physics (LASG) and Tsinghua University (CESS)  | O   | O   | X   | O   |
| MIROC-ESM <sup>113</sup>           | University of Tokyo, National Institute for Environmental Studies and Japan Agency for Marine-Earth Science and Technology  | O   | O   | O   | O   |
| MIROC-ESM-CHEM <sup>113</sup>      |   | O   | O   | O   | O   |
| MIROC-MIROC5 <sup>114</sup>        |   | O   | O   | O   | O   |
| MOHC-HadGEM2-CC <sup>115,116</sup> | UK Met Office Hadley Centre   | X   | O   | X   | O   |
| MOHC-HadGEM2-ES <sup>115,116</sup> |   | O   | O   | O   | O   |
| MPI-ESM-LR <sup>117</sup>          | Max Planck Institute for Meteorology  | O   | O   | X   | O   |
| MPI-ESM-MR <sup>117</sup>          |   | O   | X   | X   | O   |
| MRI-CGCM3 <sup>118,119</sup>       | Meteorological Research Institute   | O   | O   | O   | O   |
| NCAR-CCSM4 <sup>120</sup>          | US National Centre for Atmospheric Research   | O   | O   | O   | O   |
| NCC-NorESM1-M <sup>121</sup>       | Norwegian Climate Centre  | O   | O   | O   | O   |
| NIMR-HADGEM2-AO <sup>115,116</sup> | National Institute of Meteorological Research and Korea Meteorological Administration                                       | O   | O   | O   | O   |
| Total                              |   | 26  | 31  | 19  | 33  |

**Table 1.** CMIP5 Global Climate Models.

future period. The future periods are: 2020–2049 (2030s), 2040–2069 (2050s), 2060–2089 (2070s) and 2070–2099 (2080s). For each future period, we calculated the anomaly (delta change) with respect to the baseline climate of the same GCM for each variable and month. We used absolute differences for temperatures (Eq. 1) and relative changes for precipitation (Eq. 2).

$$\Delta X_i = X_{Fi} - X_{Ci} \quad (1)$$

$$\Delta X_i = \frac{X_{Fi} - X_{Ci}}{X_{Ci}} \quad (2)$$

where,  $\Delta X_i$  is the delta change,  $X_{Ci}$  the 30-year mean of the variable in the current climate, and  $X_{Fi}$  the 30-year mean of the variable in the future climate of each GCM in the month  $i$ .

The use of relative changes for precipitation avoids arriving at negative values when applying GCM delta values onto observed WorldClim precipitation. We note that in very dry areas (i.e. monthly historical precipitation close to zero) relative changes could produce unreasonably large relative precipitation increases (e.g. Sahara Desert). To avoid this, we made two adjustments: (1) we set a threshold of 0.1 mm month<sup>-1</sup> both for current and future GCM values, which prevents indetermination in Eq. 2; and (2) we truncate the top 2% of anomaly values to the 98<sup>th</sup> percentile value in the empirical probability distribution for each anomaly gridded dataset. Truncation

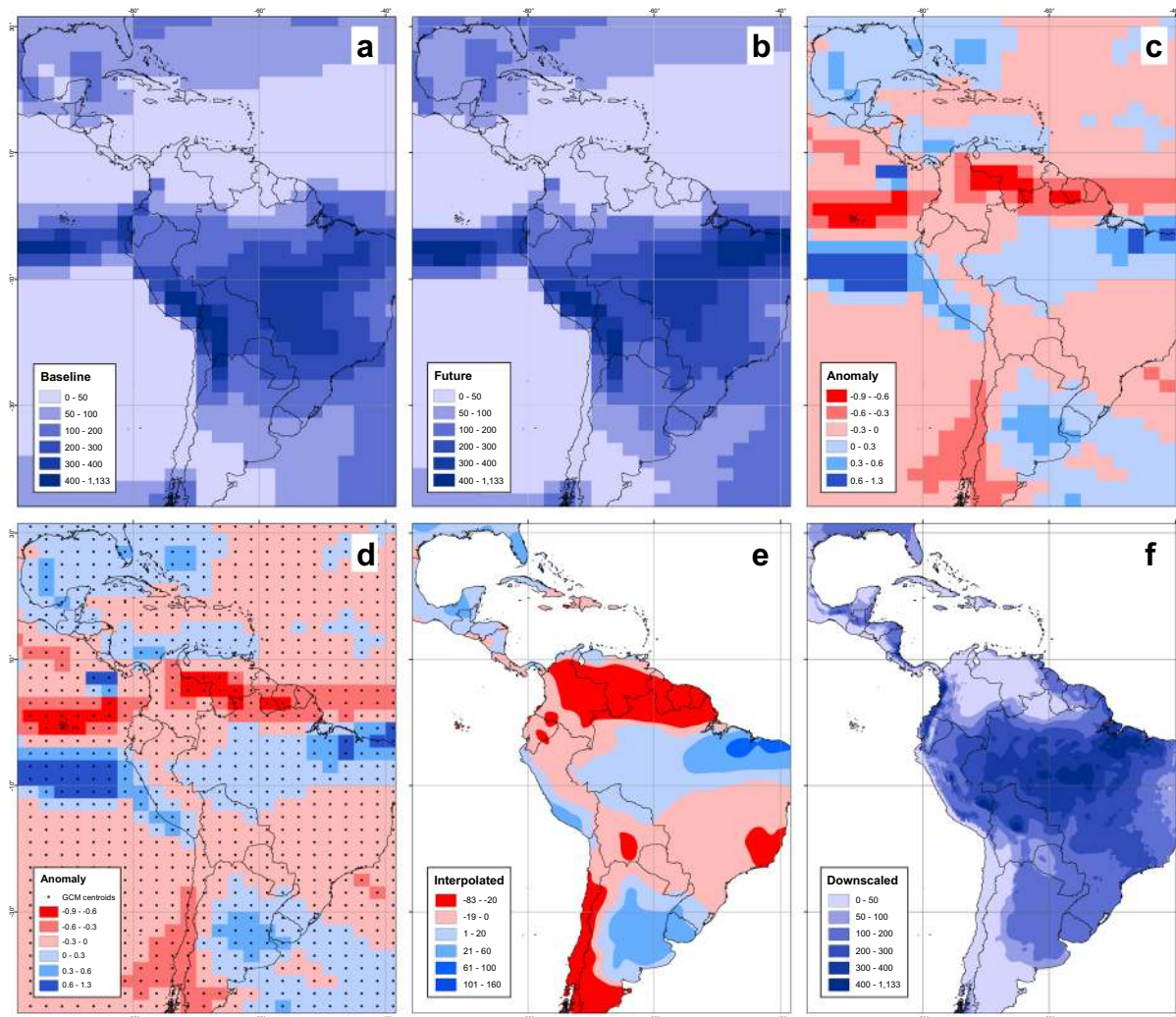


**Fig. 1** Illustration of the downscaling process with January total precipitation using the GFDL-CM3 GCM pattern. (a) Baseline data, (b) future data for 2050s (2040–2069 average), (c) delta or anomaly by 2050s, (d) delta or anomaly by 2050s with GCM centroids (points) overlaid, (e) 30 arc-s interpolated anomaly, and (f) future downscaled climate surface at 30 arc-second spatial resolution. Values in mm/month.

avoids situations in which very low values in the denominator in Eq. 2 lead to very high delta values, which when applied onto WorldClim may lead to unrealistically high values for the future precipitation.

We next apply a thin-plate splines interpolation (TPS)<sup>51,52</sup> to derive 30 arc-s anomalies. TPS have been used extensively in climate science<sup>11,46,53,54</sup>. The procedure ensures a smooth (continuous and differentiable) surface together with continuous, first-derivative surfaces. Rapid changes in gradient or slope (the first derivative) may occur in the vicinity of the data points. The spline method performs a two-dimensional minimum curvature spline interpolation on a point dataset resulting in a smooth surface that passes exactly through the input points.

Original GCM grid cells are transformed to points with position equal to the centroid of the grid cell, and the TPS interpolation is applied across these points. We used 8 points as neighborhood, though using less (4) or more (12) produced similar results. Interpolations at coastlines are done using relevant ocean grid points from the GCM, only when strictly necessary. The resolution of the resulting interpolation is 30 arc-s, for consistency with WorldClim. This interpolation procedure yields surfaces of changes in climates for each of the 12 months and 3 variables. We produce a total of 36 interpolated surfaces of monthly changes in climates per GCM, RCP and period.

We add anomalies to the baseline climates from WorldClim to get the downscaled future. In the case of temperatures (minimum and maximum temperatures) for each pixel, the anomalies in degree Celsius are simply summed to the actual value in degree Celsius reported in WorldClim (Eq. 3). For precipitation, we use the absolute value of the change relative to the baseline period in order to avoid monthly precipitation values going below 0, and maintain homogeneities with WorldClim (Eq. 4).

$$X_{DCi} = X_{OBSi} + \Delta X_{fi} \quad (3)$$



| Variable name | Description  | Units |
|---------------|--|-------|
| bio_1         | Annual mean temperature                              | °C    |
| bio_2         | Mean Diurnal Range                                   | °C    |
| bio_3         | Isothermality  | —     |
| bio_4         | Temperature Seasonality                              | °C    |
| bio_5         | Max Temperature of Warmest Month                     | °C    |
| bio_6         | Min Temperature of Coldest Month                     | °C    |
| bio_7         | Temperature Annual Range                             | °C    |
| bio_8         | Mean Temperature of Wettest Quarter                  | °C    |
| bio_9         | Mean Temperature of Driest Quarter                   | °C    |
| bio_10        | Mean Temperature of Warmest Quarter                  | °C    |
| bio_11        | Mean Temperature of Coldest Quarter                  | °C    |
| bio_12        | Total annual precipitation                           | mm    |
| bio_13        | Precipitation of Wettest Month                       | mm    |
| bio_14        | Precipitation of Driest Month                        | mm    |
| bio_15        | Precipitation Seasonality (Coefficient of Variation) | mm    |
| bio_16        | Precipitation of Wettest Quarter                     | mm    |
| bio_17        | Precipitation of Driest Quarter                      | mm    |
| bio_18        | Precipitation of Warmest Quarter                     | mm    |
| bio_19        | Precipitation of Coldest Quarter                     | mm    |

**Table 2.** List of bioclimatic variables derived from monthly data.

$$X_{DCi} = X_{OBSi} * (1 + \Delta X_{fi}) \quad (4)$$

where,  $X_{OBSi}$  is the current climate from observations (i.e. WorldClim);  $\Delta X_{fi}$  is the interpolated anomaly (delta); and  $X_{DCi}$  is the downscaled future climate of each GCM in the month  $i$ .

After calculating the corresponding future values for each of the 36 interpolated surfaces, we calculate mean temperatures, assuming a normal distribution in temperatures during the day, as the average of maximum and minimum temperatures.

Beyond the monthly data, we also calculated 19 bioclimatic indices<sup>55,56</sup> (see full list in Table 2), which have become standard for species distributions modeling for wild and crop species<sup>57,58</sup>. These indices provide descriptions of annual trends (i.e. annual mean temperature, total annual rainfall), seasonality (temperature range, temperature and precipitation standard deviations), and stressful conditions (precipitation during dry or wet periods, temperatures during hot and cold periods).

### Data Records

Our datasets comprise the most comprehensive bias-corrected set of climate change scenarios from IPCC AR5. The DC approach was applied over 35 different GCM outputs (Table 1) from CMIP5<sup>39,50</sup>, four RCPs, and four different 30-year periods, including: 2030s (2020–2049), 2050s (2040–2069), 2060s (2050–2079) and 2080s (2070–2099). The combination of all these settings produce a total of 436 different global scenarios. Each scenario comprises four variables at a monthly time-step: mean, maximum, minimum temperature, and total precipitation, in addition to a set of 19 bioclimatic variables. We provide data at four spatial resolutions, namely, 30 arc-s (~1 km at the Equator), 2.5 arc-min (~5 km), 5 arc-min (~10 km), and 10 arc-min (~20 km). We pack the twelve months of the year for each variable and resolution in Zip archives containing ESRI-Arc/Info binary grids (for 2.5, 5 and 10 arc-min datasets) and ESRI-ASCII grids (all resolutions). Moreover, we offer datasets by tiles (18 tiles in total) to facilitate the data retrieval for users who seek only regional data. All the possible combinations produce 57,552 records which are freely available in a digital table<sup>59</sup>. The complete dataset set is ~7 TB in size. All data are freely available at the World Data Center for Climate (WDCC) repository<sup>41</sup>.

### Technical Validation

The DC strategy focuses on identifying the aspects of the climate model that need correction (in our case the long-term mean), and then uses the observations to find a correction factor for the quantities of interest (e.g. long-term average monthly mean temperature). To illustrate the method, a comparison of the Probability Density Function (PDF) between observations, GCM-historical, GCM-future, and downscaled data is shown in Fig. 2 for precipitation and 3 for temperature, respectively. We chose for this example the highest emission scenario RCP 8.5 which displays greater differences than other scenarios and 2050s –a period of importance for adaptation and policy-making decisions in agriculture both from an adaptation and mitigation perspective, as it is the period around which global mean temperature is projected to exceed 2 °C above pre-industrial levels<sup>60–63</sup>.

The DC approach changes much of the distribution of the mean seasonal temperature and seasonal rainfall in the majority of the world zones studied. In areas such as Australia and New Zealand, South America and Southeast Asia, the DC approach makes both the mean, the variance and the overall PDF distribution more consistent with that of WorldClim. In the Caribbean, Melanesia, Southern Africa, the method appears to correct the systematic underestimation of seasonal rainfall under 500 mm (Fig. 2). These high-frequency and low-intensity

events are frequently referred to as the ‘drizzle problem’ in GCMs<sup>34,64,65</sup>. In Central America, GCMs tend to overestimate the distribution of rainfall values under 500 mm but also are not capable of simulating rainfall above 500 mm. In that case, the DC method modifies the variance, bringing it closer to that of WorldClim, although it can introduce some extreme high values that are unlikely to occur.

As for precipitation, historical uncorrected GCM outputs are not capable of representing the PDF of the temperature observations in many cases (Fig. 3). For example, GCMs do not reproduce very low temperatures such as those in Eastern Europe, and low tropical temperatures (Melanesia). The DC approach brings the shape of the PDF of the future projections closer to that of the observed PDF, therefore likely reducing model error. For instance, for temperatures in the Caribbean, the mean of the PDF is changed making so that it is closer to the observations. DC also helps to reproduce very low values (e.g. Eastern and Southern Africa) that are not observable in the original GCM.

In addition to the comparison of the PDF we tested the DC method by means of a Perfect Sibling evaluation (PS)<sup>15,66</sup>. Since no observations of future climate exist, we used one GCM as pseudo-observations, to then try to predict the future evolution of that simulation using another independent simulation (Fig. 4). We selected the GFDL-ESM2M as the reference simulation (the ‘perfect sibling’ or ‘truth’) and compared with the same data from other 5 GCMs in the periods 1960–1990 and 2040–2069. *Raw* refers to the uncorrected data and DC after applying the bias-correction approach. We assessed the skill using the RMSE between the perfect sibling and the other GCMs. For this example, we selected South America, but we performed the evaluation for other regions and combinations of GCMs (Fig. 5).

Both for the example simulation and for all possible combinations, the RMSE decreases significantly applying DC compared with the uncalibrated case. For the South America region the error fluctuates between  $E = 246\text{--}387\text{ mm season}^{-1}$  in the raw case and  $E = 122\text{--}159\text{ mm season}^{-1}$  (i.e. roughly 50% lower) in the DC case for DJF seasonal precipitation, and between  $E = 2\text{--}3.5\text{ }^{\circ}\text{C season}^{-1}$  in the raw case and  $E = 0.4\text{--}1.4\text{ }^{\circ}\text{C season}^{-1}$  in the DC case for DJF seasonal mean temperature (Fig. 4). The correlation between corrected GCMs and the perfect sibling, considering all the 2,400 possible combinations (among GCMs, seasons, regions), is above 0.8 in virtually all cases (i.e. seasons, regions and GCMs) for both precipitation and temperature (Fig. 5, left). The RMSE for the same combinations is less than  $200\text{ mm season}^{-1}$  ( $1.5\text{ }^{\circ}\text{C}$ ) for more than 90% (75%) of the cases for precipitation (temperature) (Fig. 5, right).

Overall, the evaluation suggests that DC produces reliable and robust future projections of the means of climate variables for use in impact assessment. However, we note that while mean seasonal conditions play a significant role in the eco-physiology of crops and wild species<sup>45,67</sup>, there are other aspects of climate projections that influence crops and biodiversity including the frequency and intensity of drought and/or hot spells, or the occurrence 1-day extreme precipitation events<sup>15,68,69</sup>. Some of these aspects, however, are not adequately simulated by GCMs<sup>70,71</sup>. More work is thus required to develop better models that can accurately simulate these events, or that generate plausible scenarios that can then be used into agricultural and species models. Additionally, other methods of bias-correction and downscaling exist (e.g. refs. <sup>25,30,37</sup>) and can correct errors in the temporal aspects of GCM simulations. Future studies and datasets may focus exploring and comparing additional methods to DC or different implementations of DC (e.g. using different interpolation methods), especially as CMIP6 model outputs become available to the public, as different methods can produce varying results and thus add to the ‘uncertainty cascade’ in impacts modeling<sup>16,72</sup>.

## Usage Notes

**Recommendations to users.** The World Data Center for Climate (WDCC) portal provides the open access high-resolution climate data presented in this article, with an associated permanent DOI ([https://doi.org/10.26050/WDCC/CCAFS-CMIP5\\_downscaling](https://doi.org/10.26050/WDCC/CCAFS-CMIP5_downscaling))<sup>41</sup>. In addition, the CCAFS-Climate portal ([www.ccafs-climate.org](http://www.ccafs-climate.org)) also provides the data, and includes useful explanations and documentation to help users understand the technical principles of the downscaling techniques and other useful information about the data. It also includes a *Contact Us* section providing user support via e-mail and an *About Us* section with institutional information and a quick guide to citing the data in peer-reviewed publications.

We provide data at four different resolutions (30 arc-s, 2.5 arc-min, 5 arc-min, and 10 arc-min), and encourage users of these data to understand the assumptions we made in producing them. The data provided here are intended to assess the impacts of changes in the mean climate state, especially as it relates to temperatures and precipitation, and the derived bioclimatic indices. For applications concerning changes in weather characteristics, extreme events, or interannual variability, users should find other datasets or bias-correction methods that address such aspects. As a whole, our assumptions might lead to uncertainties, and therefore, we suggest that users of these data perform a detailed uncertainty analysis in order to determine if these data in fact fulfil their requirements. We caution users regarding the uncertainties involved in our processes, and in no case should users understand these projections as future predictions of climate for particular places. Rather, the data should be understood as high-resolution and bias-corrected future projections in which a compromise is made between climate model physics and scale of analysis. It is noteworthy that as progress continues in climate modelling in the next decades, we expect that downscaling and bias-correction may no longer be required for using climate model output to assess the impacts of climate change.

Processing and storage capacity in research centers making use of these datasets might also be a limiting factor when using these data. We therefore suggest research centers to download the appropriate resolution datasets that suit their studies. We note that significant differences are of course present between 30 arc-s and 10 arc-min spatial resolutions. The former is the original WorldClim resolution, providing considerable detail on climatic patterns according to orography, whilst the latter, retrieves a credible high-resolution dataset, but with less level of detail.

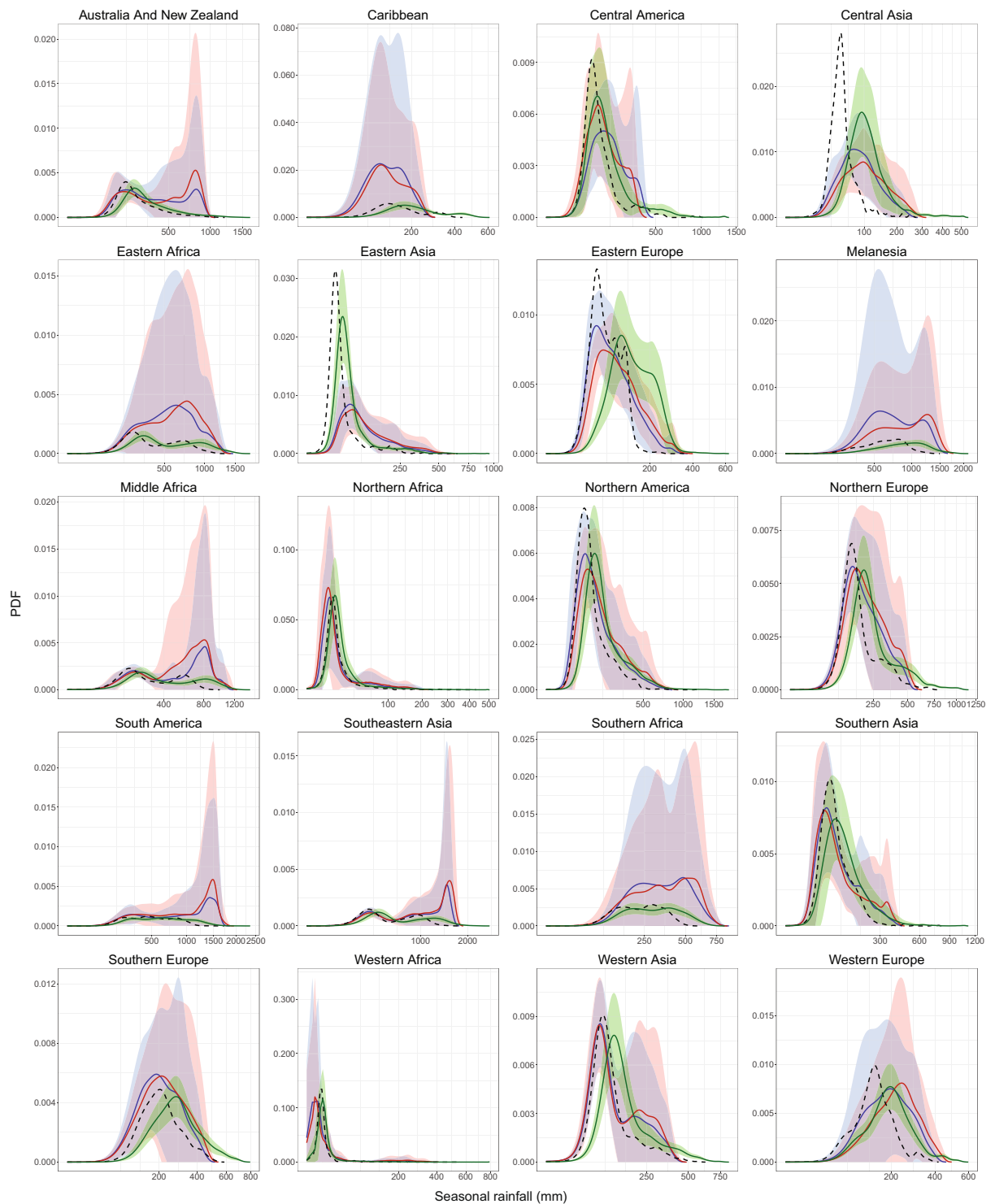


**Fig. 2** Probability density functions (PDF) of seasonal rainfall for December-January-February season in comparison with observations. The continuous lines belong to PDF average and the shading shows the average  $\pm$  one standard deviation, for all GCM-future (red), GCM-historical (blue) and DC GCM (green). Dotted line is average PDF for the observations (i.e. WorldClim). The definition of areas of the world follows the United Nations Statistics Division (UNSD)<sup>122</sup>.

**Applications in agro-environmental research.** From 2014 to date, CMIP5 DC downscaled data from the CCAFS-Climate portal have been downloaded by nearly 1,400 users in more than 186 countries around the world. Approximately 394,000 data files have been downloaded, amounting to 119 TB of data. Users of the data include representatives from national government research institutions and the NGO sector as well as the research community. Moreover, to date more than 300 journal papers, 10 book chapters, and 40 theses or reports

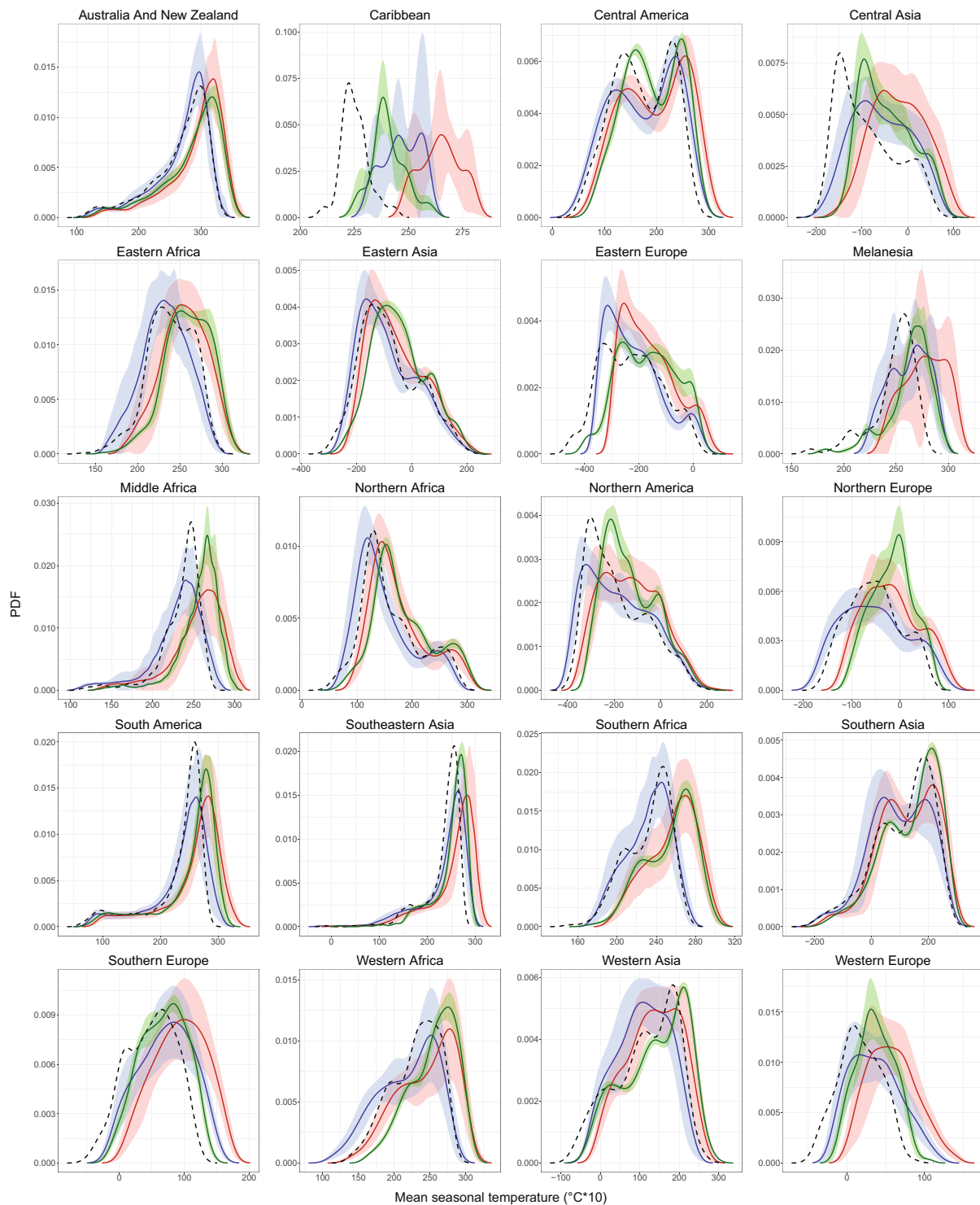


**Fig. 3** Probability density functions (PDF) of seasonal mean temperature for DJF season in comparison with observations. The continuous lines belong to PDF average and the shading shows the average  $\pm$  one standard deviation, for all GCM-future (red), GCM-historical (blue) and DC GCM (green). Dotted line is average PDF for the observations (i.e. WorldClim). The x-axis is multiplied by 10 for consistency with the data provided online, which is multiplied by 10 to reduce storage space needs. The definition of areas of the world follows the United Nations Statistics Division (UNSD)<sup>122</sup>.

have cited the data shown here. These data have been used for a wide variety of purposes; some examples are summarized below.

Guo *et al.*<sup>73</sup> used DC data to investigate the current status and distribution of the Quiver tree *Aloe dichotoma* in southern Africa and assess the projected future changes of its habitat under different climatic scenarios. The



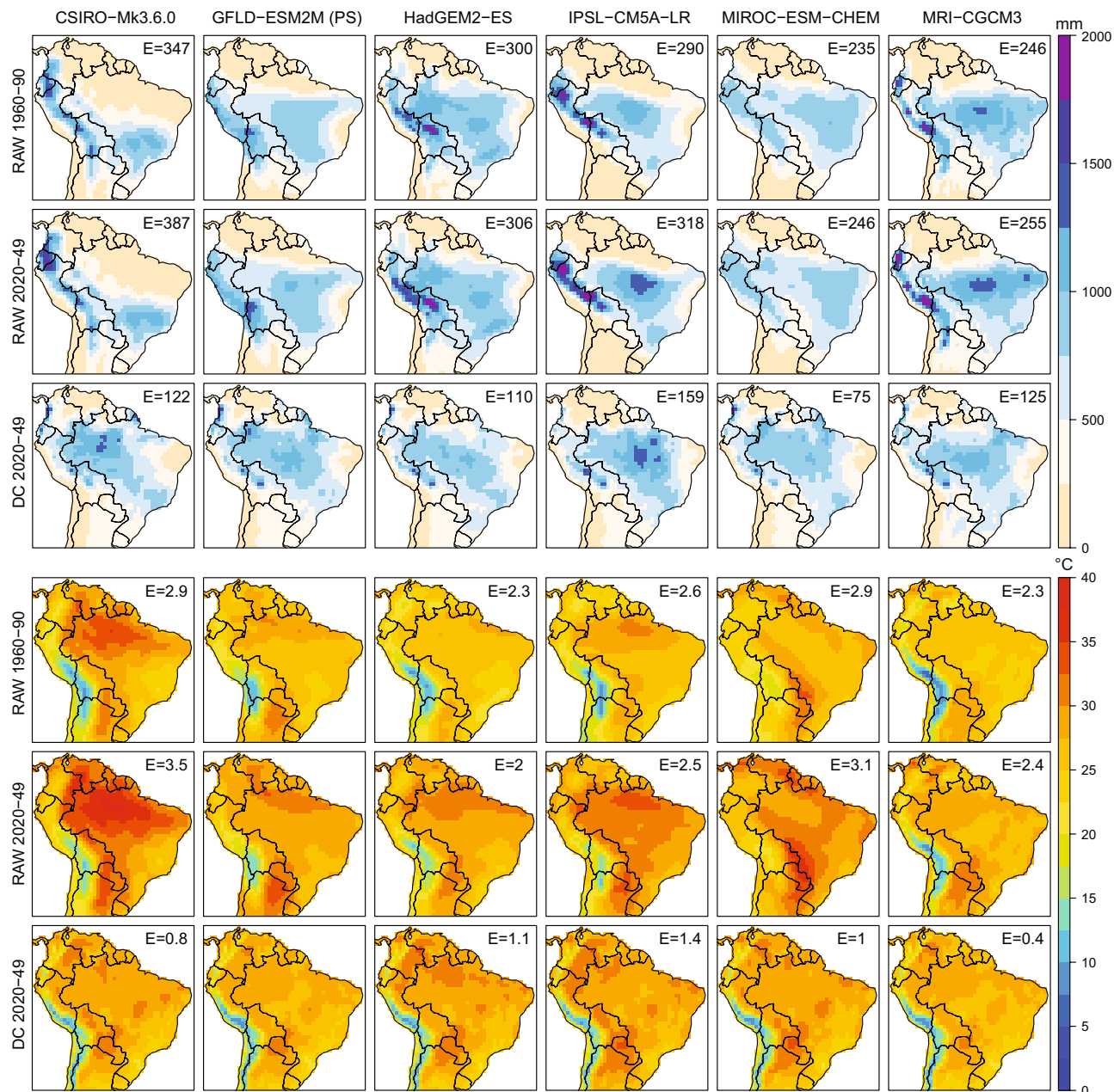


**Fig. 4** Demonstration of the DC calibration methodology using a range of GCM simulations. Top maps (in blue color scale) show results for DJF seasonal rainfall, and bottom maps (in rainbow color scale) for DJF mean seasonal temperature. GFDL-ESM2M is selected as the “perfect sibling” for verification against the calibrated projections using other GCM data. The RMS error for the region shown is given as the E value in the top-right of the maps.

tree provides moisture to a wide variety of mammals, birds and insects, and its conservation is critical to maintaining the local ecosystem in the future. Jennings and Harris<sup>74</sup> used DC data to identify specific climate and vegetation parameters for anticipating how, where and when ecosystem vegetation may transform with climate change across the southwestern USA. CCAFS-Climate portal data were used in conjunction with a weather generator to map environmental suitability for the Zika virus, showing that over 2.17 billion people in the tropics and sub-tropics live in areas suitable for the virus and its vector<sup>75</sup>.

The CCAFS-Climate portal data have been widely used to help identify analogue sites. Comparing present-day farming systems with their future analogues can facilitate the exchange of knowledge between farmers in different locations who share common climate interests and allows adaptation strategies and technologies to be tested and validated<sup>76</sup>. Over the last several years, more than 15,000 farmers have been testing new seed varieties in seven districts of India as a component of improved local seed systems, by selecting and testing varieties identified using climate analogue analysis, thereby enhancing smallholders’ resilience to climate change<sup>77</sup>. In another example, the

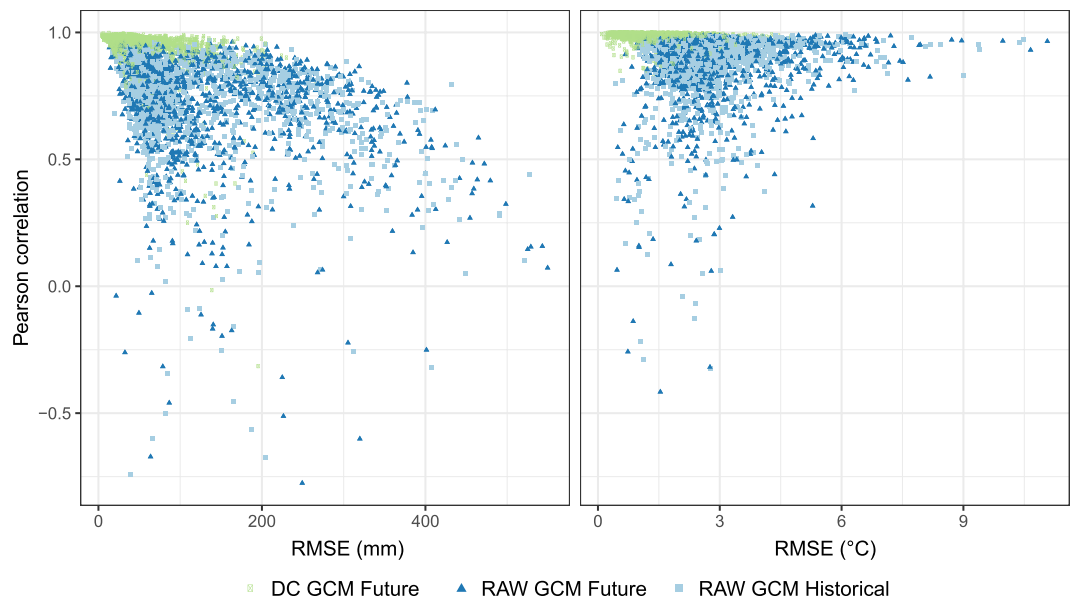


**Fig. 5** Error evaluation considering all seasons, regions and different combinations of the “Perfect Sibling” model. Left panel shows precipitation, and right panel temperature. Model error, measured using the RMSE and Pearson correlation coefficient are shown for the uncorrected GCMs in the historical period (light blue squares), the uncorrected GCMs in the future (dark blue triangles) and DC calibrated dataset (green circles).

International NGO Concern Worldwide is using analogue analysis to identify adaptation options and investment strategies in Chad and South Sudan<sup>77</sup>.

Many studies have used the CCAFS-Climate portal data to project the impacts of climate change on agricultural production. Several examples are included in working papers for crop production<sup>78</sup>, and for livestock production<sup>79</sup>, both focused on sub-Saharan Africa. In Timor Leste, government response to the 2016 El Niño included committing US\$12 million to buy reserve food stocks, partly as a result of the use of CCAFS-Climate data<sup>77</sup>. Other study<sup>80</sup> assessed the impact of global warming on outdoor ice-skating in Canada, and showed that its availability and benefits are projected to continue declining at an accelerated rate, posing a real challenge to this popular cultural ecosystem service.

CMIP5 DC data has also contributed as a main input of agriculture sector-specific studies performed in Africa. It includes an analysis of the impacts of climate change on cocoa in Ghana and Cote d’Ivoire<sup>81</sup>, the climate change impacts and potential benefits of drought and heat tolerance in chickpea in East Africa<sup>82</sup>, simulate impacts of climate change on water use and yield of irrigated sugarcane in South Africa<sup>83</sup>, potential benefits of drought and heat tolerance in groundnut for adaptation to climate change in West Africa<sup>84</sup>, analysis and mapping of climate change risk and vulnerability in Central Rift Valley of Ethiopia<sup>85</sup>, study of matching seeds to needs-female farmers adapt to a changing climate in Ethiopia<sup>86</sup>, among others.

A recent outcome assessment based on Outcome Harvesting<sup>87</sup> shows that the data in the CCAFS-Climate portal are not only widely used in research activities but are also effective in contributing to development outcomes. The climate data are influencing, directly or indirectly, a range of societal actors, including funders investing in further research, NGOs and government agencies changing their programming and planning for climate change adaptation, and farmers and communities adopting new agricultural practices. The CCAFS-Climate portal is providing scientific, robust and credible climate information, but there are also secondary functions that are contributing to the achievement of outcomes, such as supporting visualization and communication about future climates, enhancing reflective and independent thinking, and engaging partners and stakeholders in collaborative activities<sup>77</sup>.

### Code availability

The DC code used to produce the global database of future climates is publicly available under a Creative Commons Attribution 4.0 International license (CC BY 4.0). We carried out the procedure mainly in ArcInfo Workstation 10, and the R language for statistical computing<sup>88</sup>. The source code consists of two Arc Macro Language (AML)<sup>89</sup> (version 10.0) and two R (version 3.2.4) programming language scripts<sup>90</sup>.

Received: 9 April 2019; Accepted: 3 December 2019;

Published online: 20 January 2020

### References

- Gleckler, P. J., Taylor, K. E. & Doutriaux, C. Performance metrics for climate models. *J. Geophys. Res.* **113**, D06104 (2008).
- Olesen, J. *et al.* Uncertainties in projected impacts of climate change on European agriculture and terrestrial ecosystems based on scenarios from regional climate models. *Clim. Change* **81**, 123–143 (2007).

3. Challinor, A. J. *et al.* Improving the use of crop models for risk assessment and climate change adaptation. *Agric. Syst.* **159**, 296–306 (2018).
4. Baron, C. *et al.* From GCM grid cell to agricultural plot: scale issues affecting modelling of climate impact. *Philos. Trans. R. Soc. B Biol. Sci.* **360**, 2095–2108 (2005).
5. Challinor, A. J. *et al.* Methods and resources for climate impacts research. *Bull. Am. Meteorol. Soc.* **90**, 836–848 (2009).
6. Adam, M., Van Bussel, L. G. J., Leffelaar, P. A., Van Keulen, H. & Ewert, F. Effects of modelling detail on simulated potential crop yields under a wide range of climatic conditions. *Ecol. Modell.* **222**, 131–143 (2011).
7. Hoogenboom, G. *et al.* *Crop Models. Decision Support System for Agrotechnology Transfer, Version 3.0 (DSSAT V3.0), vol. 2–2. International Benchmark Sites Network for Agrotechnology Transfer (IBSNAT) Project.* (University of Hawaii, Department of Agronomy and Soil Science, 1994).
8. Buytaert, W. *et al.* Uncertainties in climate change projections and regional downscaling: implications for water resources management. *Hydrol. Earth Syst. Sci. Discuss.* **7**, 1821–1848 (2010).
9. Hewitson, B. C. & Crane, R. G. Consensus between GCM climate change projections with empirical downscaling: precipitation downscaling over South Africa. *Int. J. Climatol.* **26**, 1315–1337 (2006).
10. Jacob, D. *et al.* An inter-comparison of regional climate models for Europe: model performance in present-day climate. *Clim. Change* **81**, 31–52 (2007).
11. Hijmans, R. J., Cameron, S. E., Parra, J. L., Jones, P. G. & Jarvis, A. Very high resolution interpolated climate surfaces for global land areas. *Int. J. Climatol.* **25**, 1965–1978 (2005).
12. Wilby, R. L. *et al.* A review of climate risk information for adaptation and development planning. *Int. J. Climatol.* **29**, 1193–1215 (2009).
13. Baigorria, G. A., Jones, J. W. & O'Brien, J. J. Potential predictability of crop yield using an ensemble climate forecast by a regional circulation model. *Agric. For. Meteorol.* **148**, 1353–1361 (2008).
14. Challinor, A. J., Wheeler, T. R., Craufurd, P. Q. & Slingo, J. M. Simulation of the impact of high temperature stress on annual crop yields. *Agric. For. Meteorol.* **135**, 180–189 (2005).
15. Hawkins, E., Osborne, T. M., Ho, C. K. & Challinor, A. J. Calibration and bias correction of climate projections for crop modelling: an idealised case study over Europe. *Agric. For. Meteorol.* **170**, 19–31 (2013).
16. Quintana Seguí, P., Ribes, A., Martin, E., Habets, F. & Boé, J. Comparison of three downscaling methods in simulating the impact of climate change on the hydrology of Mediterranean basins. *J. Hydrol.* **383**, 111–124 (2010).
17. Zhang, X. C. Spatial downscaling of global climate model output for site-specific assessment of crop production and soil erosion. *Agricultural and Forest Meteorology* **135**, 215–229 (2005).
18. Jones, P. G. & Thornton, P. Generating downscaled weather data from a suite of climate models for agricultural modelling applications. *Agric. Syst.* **114**, 1–5 (2013).
19. Tabor, K. & Williams, J. W. Globally downscaled climate projections for assessing the conservation impacts of climate change. *Ecol. Appl.* **20**, 554–565 (2010).
20. Jarvis, A., Lane, A. & Hijmans, R. J. The effect of climate change on crop wild relatives. *Agric. Ecosyst. Environ.* **126**, 13–23 (2008).
21. Musau, J., Sang, J. & Gathenya, J. General Circulation Models (GCMs) Downscaling Techniques and Uncertainty Modeling for Climate Change Impact Assessment. *Proceedings of Sustainable Research and Innovation Conference, [S.I.]*, p. 147–153, ISSN 2079-6226 (2014).
22. Rummukainen, M. State-of-the-art with regional climate models. *Wiley Interdiscip. Rev. Chang.* **1**, 82–96 (2010).
23. Ramirez-Villegas, J. & Challinor, A. Assessing relevant climate data for agricultural applications. *Agric. For. Meteorol.* **161**, 26–45 (2012).
24. White, J. W., Hoogenboom, G., Kimball, B. A. & Wall, G. W. Methodologies for simulating impacts of climate change on crop production. *F. Crop. Res.* **124**, 357–368 (2011).
25. Ehret, U., Zehe, E., Wulfmeyer, V., Warrach-Sagi, K. & Liebert, J. Should we apply bias correction to global and regional climate model data? *Hydrol. Earth Syst. Sci. Discuss.* **9**, 5355–5387 (2012).
26. Maurer, E. P. & Hidalgo, H. G. Utility of daily vs. monthly large-scale climate data: an intercomparison of two statistical downscaling methods. *Hydrol. Earth Syst. Sci.* **12**, 551–563 (2008).
27. Jones, R. *et al.* *Generating high resolution climate change scenarios using PRECIS.* (Met Office Hadley Centre, 2004).
28. Xu, Z. & Yang, Z.-L. A new dynamical downscaling approach with GCM bias corrections and spectral nudging. *J. Geophys. Res. Atmos.* **120**, 2014JD022958 (2015).
29. Garcia-Carreras, L. *et al.* The Impact of Parameterized Convection on the Simulation of Crop Processes. *J. Appl. Meteorol. Climatol.* **54**, 1283–1296 (2015).
30. Wilby, R. L. & Wigley, T. M. L. Downscaling general circulation model output: a review of methods and limitations. *Prog. Phys. Geogr.* **21**, 530–548 (1997).
31. Giorgi, F., Jones, C. & Asrar, G. R. Addressing climate information needs at the regional level: the CORDEX framework. *World Meteorol. Organ. Bull.* **58**, 175–183 (2009).
32. Kendon, E. J., Jones, R. G., Kjellström, E. & Murphy, J. M. Using and Designing GCM-RCM Ensemble Regional Climate Projections. *J. Clim.* **23**, 6485–6503 (2010).
33. Sørland, S. L., Schär, C., Lüthi, D. & Kjellström, E. Bias patterns and climate change signals in GCM-RCM model chains. *Environ. Res. Lett.* **13**, 074017 (2018).
34. Maraun, D. Bias Correction, Quantile Mapping, and Downscaling: Revisiting the Inflation Issue. *J. Clim.* **26**, 2137–2143 (2013).
35. Gebrechorkos, S. H., Hülsmann, S. & Bernhofer, C. Statistically downscaled climate dataset for East Africa. *Sci. Data* **6**, 31 (2019).
36. Wilby, R., Charles, S., Zorita, E. & Timbal, B. Guidelines for use of climate scenarios developed from statistical downscaling methods. *Supporting material of the Intergovernmental Panel on Climate Change, available from the DDC of IPCC TG CIA 27* (2004).
37. Themeßl, J. M., Gobiet, A. & Leuprecht, A. Empirical-statistical downscaling and error correction of daily precipitation from regional climate models. *Int. J. Climatol.* **31**, 1530–1544 (2011).
38. Ines, A. V. M., Hansen, J. W. & Robertson, A. W. Enhancing the utility of daily GCM rainfall for crop yield prediction. *Int. J. Climatol.* **31**, 2168–2182 (2011).
39. Taylor, K. E., Stouffer, R. J. & Meehl, G. A. An Overview of CMIP5 and the Experiment Design. *Bull. Am. Meteorol. Soc.* **93**, 485–498 (2012).
40. Moss, R. H. *et al.* The next generation of scenarios for climate change research and assessment. *Nature* **463**, 747–756 (2010).
41. Navarro-Racines, C. E., Tarapues-Montenegro, J. E., Thornton, P., Jarvis, A. & Ramirez-Villegas, J. CCAFS-CMIP5 Delta Method Downscaling for monthly averages and bioclimatic indices of four RCPs. *World Data Center for Climate (WDCC) at DKRZ.*, [https://doi.org/10.26050/WDCC/CCAFS-CMIP5\\_downscaling](https://doi.org/10.26050/WDCC/CCAFS-CMIP5_downscaling) (2019).
42. Ho, C. K., Stephenson, D. B., Collins, M., Ferro, C. A. T. & Brown, S. J. Calibration strategies; a source of additional uncertainty in climate change projections. *Bull. Am. Meteorol. Soc.* **93**, 21–26 (2012).
43. Hay, L. E., Wilby, R. L. & Leavesley, G. H. A comparison of delta change and downscaled GCM scenarios for three mountainous basins in the United States. *JAWRA J. Am. Water Resour. Assoc.* **36**, 387–397 (2000).
44. Rippke, U. *et al.* Timescales of transformational climate change adaptation in sub-Saharan African agriculture. *Nat. Clim. Chang.* **6**, 605–609 (2016).

45. Warren, R. *et al.* Quantifying the benefit of early climate change mitigation in avoiding biodiversity loss. *Nat. Clim. Chang.* **3**, 678–682 (2013).
46. Hutchinson, M. F. Interpolating mean rainfall using thin plate smoothing splines. *Int. J. Geogr. Inf. Syst.* **9**, 385–403 (1995).
47. Harris, I., Jones, P. D., Osborn, T. J. & Lister, D. H. Updated high-resolution grids of monthly climatic observations – the CRU TS3.10 Dataset. *Int. J. Climatol.* **34**, 623–642 (2014).
48. Deblauwe, V. *et al.* Remotely sensed temperature and precipitation data improve species distribution modelling in the tropics. *Glob. Ecol. Biogeogr.* **25**, 443–454 (2016).
49. Funk, C. *et al.* The climate hazards infrared precipitation with stations—a new environmental record for monitoring extremes. *Sci. Data* **2**, 150066 (2015).
50. IPCC. Climate Change 2013 The Physical Science Basis Working Group I Contribution to the Fifth Assessment Report of the Intergovernmental Panel on Climate Change [Stocker, T. F. *et al.*] *Cambridge Univ. Press United Kingdom New York, NY, USA* 1535 pp (2013).
51. Franke, R. Smooth interpolation of scattered data by local thin plate splines. *Comput. Math. with Appl.* **8**, 273–281 (1982).
52. Mitáš, L. & Mitášová, H. General variational approach to the interpolation problem. *Comput. Math. with Appl.* **16**, 983–992 (1988).
53. Hutchinson, M. F. *A summary of some surface fitting and contouring programs for noisy data.* (1984).
54. Hutchinson, M. F. & de Hoog, F. R. Smoothing noisy data with spline functions. *Numer. Math.* **47**, 99–106 (1985).
55. Nix, H. A. *A biogeographic analysis of Australian elapid snakes. Atlas of Elapid Snakes of Australia* (Australian Government Publishing Service: Canberra, 1986).
56. Busby, J. R. BIOCLIM—a bioclimate analysis and prediction system. *Plant Prot. Q.* **6**, 8–9 (1991).
57. Khoury, C. K. *et al.* Comprehensiveness of conservation of useful wild plants: An operational indicator for biodiversity and sustainable development targets. *Ecol. Indic.* **98**, 420–429 (2019).
58. Castro-Llanos, F., Hyman, G., Rubiano, J., Ramirez-Villegas, J. & Achicanoy, H. Climate change favors rice production at higher elevations in Colombia. *Mitig. Adapt. Strateg. Glob. Chang.* <https://doi.org/10.1007/s11027-019-09852-x> (2019).
59. Navarro-Racines, C., Tarapues-Montenegro, J., Guevara, E., Jarvis, A. & Ramirez-Villegas, J. CCAFS-CMIP5 Delta Method Downscaling database. [figshare, https://doi.org/10.6084/m9.figshare.5239615.v6](https://doi.org/10.6084/m9.figshare.5239615.v6) (2019).
60. Nelson, G. C. *et al.* *Food Security, Farming and Climate Change to 2050: Scenarios, Results and Policy Options.* (International Food Policy Research Institute, 2010).
61. Grafton, R. Q., Daugbjerg, C. & Qureshi, M. E. Towards food security by 2050. *Food Secur.* **7**, 179–183 (2015).
62. Rogelj, J. *et al.* Paris Agreement climate proposals need a boost to keep warming well below 2°C. *Nature* **534**, 631–639 (2016).
63. Schleussner, C.-F. *et al.* Differential climate impacts for policy-relevant limits to global warming: the case of 1.5°C and 2°C. *Earth Syst. Dyn.* **7**, 327–351 (2016).
64. DeFlorio, M. J., Pierce, D. W., Cayan, D. R. & Miller, A. J. Western U.S. Extreme Precipitation Events and Their Relation to ENSO and PDO in CCSM4. *J. Clim.* **26**, 4231–4243 (2013).
65. Wang, Y., Zhang, G. J. & Craig, G. C. Stochastic convective parameterization improving the simulation of tropical precipitation variability in the NCAR CAM5. *Geophys. Res. Lett.* **43**, 6612–6619 (2016).
66. Hawkins, E. *et al.* Increasing influence of heat stress on French maize yields from the 1960s to the 2030s. *Glob. Chang. Biol.* **19**, 937–947 (2013).
67. Läderach, P. *et al.* Climate change adaptation of coffee production in space and time. *Clim. Change* **141**, 47–62 (2017).
68. Katz, R. W. & Brown, B. G. Extreme events in a changing climate: Variability is more important than averages. *Clim. Change* **21**, 289–302 (1992).
69. Field, C. B. *et al.* *Managing the Risks of Extreme Events and Disasters to Advance Climate Change Adaptation. A Special Report of Working Groups I and II of the Intergovernmental Panel on Climate Change.* <https://doi.org/10.1017/CBO9781139177245>, (Cambridge University Press, 2012).
70. Sillmann, J., Kharin, V. V., Zhang, X., Zwiers, F. W. & Bronaugh, D. Climate extremes indices in the CMIP5 multimodel ensemble: Part I. Model evaluation in the present climate. *J. Geophys. Res. Atmos.* **118**, 1716–1733 (2013).
71. Ramirez-Villegas, J., Challinor, A. J., Thornton, P. K. & Jarvis, A. Implications of regional improvement in global climate models for agricultural impact research. *Environ. Res. Lett.* **8**, 24018 (2013).
72. Koehler, A.-K., Challinor, A. J., Hawkins, E. & Asseng, S. Influences of increasing temperature on Indian wheat: quantifying limits to predictability. *Environ. Res. Lett.* **8**, 34016 (2013).
73. Guo, D., Arnolds, J. L., Midgley, G. F. & Foden, W. B. Conservation of Quiver Trees in Namibia and South Africa under a Changing Climate. *J. Geosci. Environ. Prot.* **04**, 1–8 (2016).
74. Jennings, M. D. & Harris, G. M. Climate change and ecosystem composition across large landscapes. *Landsc. Ecol.* **32**, 195–207 (2017).
75. Messina, J. P. *et al.* Mapping global environmental suitability for Zika virus. *Elife* **5** (2016).
76. Jarvis, A. *et al.* Farms of the future: An innovative approach for strengthening adaptive capacity. In *International Conference on Agricultural Innovation Systems in Africa (ASIA)*. <https://doi.org/10.13140/2.1.1269.9208> (2013).
77. Rassmann, K. & Schuetz, T. An assessment of the influence of CCAFS’ climate data and tools on outcomes achieved 2010–2016. *CCAFS outcomes evaluation report 1* (2017).
78. Ramirez-Villegas, J. & Thornton, P. K. Climate change impacts on African crop production. *CCAFS Working Paper* (2015).
79. Thornton, P. K., Boone, R. B. & Ramirez-Villegas, J. *Climate Change Impacts on Livestock.* (2015).
80. Brammer, J. R., Samson, J. & Humphries, M. M. Declining availability of outdoor skating in Canada. *Nat. Clim. Chang.* **5**, 2–4 (2015).
81. Schroth, G., Läderach, P., Martinez-Valle, A. I., Bunn, C. & Jassogne, L. Vulnerability to climate change of cocoa in West Africa: Patterns, opportunities and limits to adaptation. *Sci. Total Environ.* **556**, 231–241 (2016).
82. Singh, P. *et al.* Climate change impacts and potential benefits of drought and heat tolerance in chickpea in South Asia and East Africa. *Eur. J. Agron.* **52**, 123–137 (2014).
83. Jones, M. R., Singels, A. & Ruane, A. C. Simulated impacts of climate change on water use and yield of irrigated sugarcane in South Africa. *Agric. Syst.* **139**, 260–270 (2015).
84. Singh, P. *et al.* Potential benefits of drought and heat tolerance in groundnut for adaptation to climate change in India and West Africa. *Mitig. Adapt. Strateg. Glob. Chang.* **19**, 509–529 (2014).
85. Gizachew, L. & Shimelis, A. Analysis and mapping of climate change risk and vulnerability in Central Rift Valley of Ethiopia. *African Crop Sci. J.* **22**, 807–818 (2014).
86. Gotor, E., Fadda, C. & Trincia, C. *Matching Seeds to Needs-female farmers adapt to a changing climate in Ethiopia.* (2014).
87. Wilson-Grau, R. & Britt, H. *Outcome harvesting.* **2012** (2013).
88. R Core Team R: A language and environment for statistical computing (2018).
89. ESRI. ArcGIS ArcInfo: Release 10 (2011).
90. Navarro-Racines, C. *et al.* Delta method downscaling programming language scripts. [figshare, https://doi.org/10.6084/m9.figshare.5236471.v4](https://doi.org/10.6084/m9.figshare.5236471.v4) (2018).
91. Wu, T. A mass-flux cumulus parameterization scheme for large-scale models: description and test with observations. *Clim. Dyn.* **38**, 725–744 (2012).
92. Xin, X., Wu, T., Li, J. F., Wang, Z. & Li, W. How Well does BCC\_CSM1.1 Reproduce the 20th Century Climate Change over China? *Atmos. Ocean. Sci. Lett.* **6**, 21–26 (2012).



93. Xin, X., Zhang, L., Zhang, J., Wu, T. & Fang, Y. Climate Change Projections over East Asia with BCC\_CSM1.1 Climate Model under RCP Scenarios. *J. Meteorol. Soc. Japan. Ser. II* **91**, 413–429 (2013).
94. Ji, D. *et al.* Description and basic evaluation of Beijing Normal University Earth System Model (BNU-ESM) version 1. *Geosci. Model Dev.* **7**, 2039–2064 (2014).
95. Arora, V. K. *et al.* Carbon emission limits required to satisfy future representative concentration pathways of greenhouse gases. *Geophys. Res. Lett.* **38**, L05805 (2011).
96. von Salzen, K. *et al.* The Canadian Fourth Generation Atmospheric Global Climate Model (CanAM4). Part I: Representation of Physical Processes. *Atmosphere-Ocean* **51**, 104–125 (2013).
97. Hurrell, J. W. *et al.* The Community Earth System Model: A Framework for Collaborative. *Research. Bull. Am. Meteorol. Soc.* **94**, 1339–1360 (2013).
98. Long, M. C., Lindsay, K., Peacock, S., Moore, J. K. & Doney, S. C. Twentieth-Century Oceanic Carbon Uptake and Storage in CESM1(BGC)\*. *J. Clim.* **26**, 6775–6800 (2013).
99. Voldoire, A. *et al.* The CNRM-CM5.1 global climate model: description and basic evaluation. *Clim. Dyn.* **40**, 2091–2121 (2013).
100. Bi, D. *et al.* The ACCESS coupled model: description, control climate and evaluation. *Aust. Meteorol. Oceanogr. J.* **63**, 41–64 (2013).
101. Dix, M. *et al.* The ACCESS coupled model: documentation of core CMIP5 simulations and initial results. *Aust. Meteorol. Oceanogr. J.* **63**, 83–99 (2013).
102. Rotstayn, L. D. *et al.* Aerosol- and greenhouse gas-induced changes in summer rainfall and circulation in the Australasian region: a study using single-forcing climate simulations. *Atmos. Chem. Phys.* **12**, 6377–6404 (2012).
103. Hazeleger, W. *et al.* EC-Earth V2.2: description and validation of a new seamless earth system prediction model. *Clim. Dyn.* **39**, 2611–2629 (2012).
104. Qiao, F. *et al.* Development and evaluation of an Earth System Model with surface gravity waves. *J. Geophys. Res. Ocean.* **118**, 4514–4524 (2013).
105. Delworth, T. L. *et al.* GFDL's CM2 Global Coupled Climate Models. Part I: Formulation and Simulation Characteristics. *J. Clim.* **19**, 643–674 (2006).
106. Donner, L. J. *et al.* The Dynamical Core, Physical Parameterizations, and Basic Simulation Characteristics of the Atmospheric Component AM3 of the GFDL Global Coupled Model CM3. *J. Clim.* **24**, 3484–3519 (2011).
107. Dunne, J. P. *et al.* GFDL's ESM2 Global Coupled Climate–Carbon Earth System Models. Part II: Carbon System Formulation and Baseline Simulation Characteristics\*. *J. Clim.* **26**, 2247–2267 (2013).
108. Schmidt, G. A. *et al.* Present-Day Atmospheric Simulations Using GISS ModelE: Comparison to *In Situ*, Satellite, and Reanalysis Data. *J. Clim.* **19**, 153–192 (2006).
109. Schmidt, G. A. *et al.* Configuration and assessment of the GISS ModelE2 contributions to the CMIP5 archive. *J. Adv. Model. Earth Syst.* **6**, 141–184 (2014).
110. Volodin, E. M., Dianskii, N. A. & Gusev, A. V. Simulating present-day climate with the INMCM4.0 coupled model of the atmospheric and oceanic general circulations. *Izv. Atmos. Ocean. Phys.* **46**, 414–431 (2010).
111. Dufresne, J.-L. *et al.* Climate change projections using the IPSL-CM5 Earth System Model: from CMIP3 to CMIP5. *Clim. Dyn.* **40**, 2123–2165 (2013).
112. Li, L. *et al.* The flexible global ocean-atmosphere-land system model, Grid-point Version 2: FGOALS-g2. *Adv. Atmos. Sci.* **30**, 543–560 (2013).
113. Watanabe, S. *et al.* MIROC-ESM 2010: model description and basic results of CMIP5-20c3m experiments. *Geosci. Model Dev.* **4**, 845–872 (2011).
114. Watanabe, M. *et al.* Improved Climate Simulation by MIROC5: Mean States, Variability, and Climate Sensitivity. *J. Clim.* **23**, 6312–6335 (2010).
115. Collins, W. J. *et al.* Development and evaluation of an Earth-System model – HadGEM2. *Geosci. Model Dev.* **4**, 1051–1075 (2011).
116. Martin, G. *et al.* The HadGEM2 family of Met Office Unified Model climate configurations. *Geosci. Model Dev.* **4**, 723–757 (2011).
117. Reick, C. H., Raddatz, T., Brovkin, V. & Gayler, V. Representation of natural and anthropogenic land cover change in MPI-ESM. *J. Adv. Model. Earth Syst.* **5**, 459–482 (2013).
118. Yukimoto, S. *et al.* *Meteorological Research Institute-Earth System Model v1 (MRI-ESM1)—Model Description* (2011).
119. Yukimoto, S. *et al.* A New Global Climate Model of the Meteorological Research Institute: MRI-CGCM3: Model Description and Basic Performance. *J. Meteorol. Soc. Japan. Ser. II* **90A**, 23–64 (2012).
120. Gent, P. R. *et al.* The Community Climate System Model Version 4. *J. Clim.* **24**, 4973–4991 (2011).
121. Iversen, T. *et al.* The Norwegian Earth System Model, NorESM1-M – Part 2: Climate response and scenario projections. *Geosci. Model Dev.* **6**, 389–415 (2013).
122. United Nations Statistics Division. *Standard Country or Area Codes for Statistical Use (Rev. 3), Series M: Miscellaneous Statistical Papers, No. 49* (1996).

## Acknowledgements

This work was implemented as part of the CGIAR Research Program on Climate Change, Agriculture and Food Security (CCAFS), which is carried out with support from CGIAR Trust Fund Donors and through bilateral funding agreements. For details, please visit [www.ccafs.cgiar.org/donors](http://www.ccafs.cgiar.org/donors). The views expressed in this paper cannot be taken to reflect the official opinions of these organizations. We acknowledge the World Climate Research Programme's Working Group on Coupled Modelling, which is responsible for CMIP, and we thank the climate modeling groups (listed in Table 1) for producing and making available their model output. For CMIP, the U.S. Department of Energy's Program for Climate Model Diagnosis and Inter-comparison provides coordinating support and led the development of software infrastructure in partnership with the Global Organization for Earth System Science Portals. We gratefully acknowledge to Osana Bonilla-Findji, David Abreu, Héctor Tobón and all the Flagship 2 (Climate Smart Agricultural Practices) CCAFS team, who helped to the development of the CCAFS-Climate portal since its inception. We thank Kornelia Rassmann and Tonya Schuetz who performed an evaluation of the contribution of the portal to development outcomes and environmental impact research studies. We thank to Dr. Frank Toussaint for his help to host the data at WDCC and thank the WDCC for hosting our dataset. Finally, we thank Myles J. Fisher, emeritus scientist from CIAT, for his help with the editing of this manuscript.

## Author contributions

C.N.-R. drafted the manuscript, produced the datasets and performed their technical validation. J.T.-M. produced the datasets and performed their technical validation. P.T. drafted the manuscript. A.J. conceived the study and aided with methodological design. J.R.-V. conceived the study, drafted the manuscript, edited the manuscript and aided with methodological design. All authors have read and approved the final version of the manuscript.

## Competing interests

The authors declare no competing interests.

## Additional information

**Correspondence** and requests for materials should be addressed to J.R.-V.

**Reprints and permissions information** is available at [www.nature.com/reprints](http://www.nature.com/reprints).

**Publisher's note** Springer Nature remains neutral with regard to jurisdictional claims in published maps and institutional affiliations.



**Open Access** This article is licensed under a Creative Commons Attribution 4.0 International License, which permits use, sharing, adaptation, distribution and reproduction in any medium or format, as long as you give appropriate credit to the original author(s) and the source, provide a link to the Creative Commons license, and indicate if changes were made. The images or other third party material in this article are included in the article's Creative Commons license, unless indicated otherwise in a credit line to the material. If material is not included in the article's Creative Commons license and your intended use is not permitted by statutory regulation or exceeds the permitted use, you will need to obtain permission directly from the copyright holder. To view a copy of this license, visit <http://creativecommons.org/licenses/by/4.0/>.

The Creative Commons Public Domain Dedication waiver <http://creativecommons.org/publicdomain/zero/1.0/> applies to the metadata files associated with this article.

© The Author(s) 2020